# Hydromagnetic squeeze film behavior between longitudinally rough circular step bearing and slip velocity effect

**J. V. Adeshara[1], Dr. M. B. Prajapati[2], Dr. G. M. Deheri[3], R. M. Patel[4]**

1. Research Scholar, Department of Mathematics, H. N. G. University, Patan – 384 265, Gujarat State, India. Email: adesharajatin01@gmail.com
2. Head, Department of Mathematics, H. N. G. University, Patan – 384 265, Gujarat State, India. Email.mbpbaou@gmail.com
3. Department of Mathematics, S. P. University, Vallabh Vidyanagar – 388 120, Gujarat State, India. Email.gmdeheri@rediffmail.com
4. Department of Mathematics, Gujarat Arts and Science College, Ahmedabad - 380 006 Gujarat State, India. Email: rmpatel2711@gmail.com

* Corresponding author: rmpatel2711@gmail.com

**Abstract:**

A circular step bearing which normally approaches a parallel rough circular surface in the presence of a hydromagnetic fluid is considered by taking into account the velocity slip. Beavers and Joseph's slip model was used to study the effect velocity slip, while the stochastic averaging process of Christensen and Tonder is accountable for assessing the longitudinal effect of surface roughness. The statistically averaged equation of the Reynolds' type is solved to obtain the pressure distribution leading to the calculation of the load bearing capacity. The calculated results presented in graphical form clearly mention that the performance is suggestively improved. The effect of roughness and slip velocity is adverse in general but there are some possibilities to improve performance by choosing the suitable combination of hydromagnetization, conductivity, radii ratio and the variance (-ve) in case of negatively skewed roughness associated with longitudinal roughness.

**Key words:**

Circular step bearing, hydromagnetic fluid, longitudinal roughness, slip velocity, load carrying capacity

**Nomenclature:**

| | |
|---|---|
| $r$ | Radial coordinate |
| $r_o$ | Outer radius |
| $r_i$ | Inner radius |
| $k$ | $=\frac{r_i}{r_o}$ − Radii ratio |
| $h$ | Lubricant film thickness |
| $H$ | Thickness of solid housing |
| $s$ | Electrical conductivity of the lubricant |
| $\mu$ | Viscosity of the lubricant |
| $B_o$ | Uniform transverse magnetic field applied between the plates |
| $M$ | $= B_0 h\left(\frac{s}{\mu}\right)^{1/2}$ − Hartmann Number |
| $p_s$ | Supply Pressure |
| $Q$ | Flow rate |
| $P_s^*$ | Dimensionless supply pressure |
| $p$ | Lubricant pressure |
| $P$ | Non-dimensional pressure |
| $w$ | Load carrying capacity |
| $W$ | Dimensionless load carrying capacity |
| $h_0'$ | Surface width of lower plate |
| $h_1'$ | Surface width of upper plate |
| $s_0$ | Electrical conductivity of lower surface |

| | |
|---|---|
| $s_1$ | Electrical conductivity of upper surface |
| $\phi_0(h)$ | $=\frac{s_0 h_0'}{sh}$ − Electrical permeability of lower surface |
| $\phi_1(h)$ | $=\frac{s_1 h_1'}{sh}$ −Electrical permeability of upper surface |
| S* | Non-dimensional slip parameter |
| σ* | Non-dimensional standard deviation |
| α* | Dimensionless variance |
| ε* | Non dimensional skewness |

**Introduction:**

Murti [15] analyzed the squeeze film behavior between two circular disks when one disk had a porous facing. It was noticed that the pressure over the entire disk was reduced by an enhanced value for the permeability parameter. At very low film thickness, the porous effects were shown to predominate.. The performance of a hydromagnetic squeeze film in porous circular disks was investigated Patel and Hingu[18]. The transverse magnetic field has resulted in increased performance. Hydromagnetic squeeze film is well known to be used in braking devices for hydraulic shock absorbers and astronautical vehicles. Bhat and Deheri[4] extended and developed Murti[15] method for presenting magnetic fluid-based squeeze film in curved circular porous plates. There was a porous face on the upper disk. The magnetization effect was independent of the upper disk curvature. Deheri and Patel [9] considered a squeeze film containing ferrofluid in porous circular disks with sealed boundary. The combined effect of magnetic fluid lubricant and boundary sealing significantly increased the capacity of the load. Deheri et al. [10] studied the performance of a ferrofluid-based variable thickness squeeze film between porous circular plates. The magnetization increased the viscosity factor and the load carrying capacity increased sharply. It was also established that a magnetic fluid-based squeeze film bearing with variable porous matrix thickness could be made to perform better than a standard porous bearing with uniform porous matrix thickness.

Deheri and Abhangi[8] extended the Bhat and Deheri analysis, [4] by taking both curved surfaces. Although the roughness of the transverse surface has had an adverse effect. This investigation provided ample scope for significantly improving performance in the case of negative skewed roughness, at least, Choose the appropriate curvature parameters. Lin et al.[14] discussed the squeeze film characteristics of non-Newtonian pair stressed parallel circular disks lubricated by ferrofluids. The non-Newtonian ferrofluid lubricated squeeze film provided a higher load capacity and extended the response time compared to the Newtonian non-ferrofluid case. Beavers and Joseph[1] put forward a simple theory based on replacing the boundary-level effect with a slip velocity proportional to the exterior velocity gradient. It was found that the result obtained from this theory is in good agreement with the experimental resultsWu[13] studied the effect of velocity slip between porous rectangular plates on squeeze film lubrication. Concerning the slip velocity, the load carrying capacity and response time were found to be reduced. The effect of velocity slip on porouswalled squeeze film was investigated Sparrow et al.[27]. The use of porous materials that accentuated the velocity slip resulted in a substantially faster response.

The pinch-induced effect of axial current on squeeze film performance was analyzed with velocity slip between two annular disks Gupta and Patel[12]. The pinch effect significantly altered the squeeze film's action. The effect of slip velocity on the squeeze film between rotating porous annular disks was discussed Prakash and Vij[25]. The effect of slip was found to be adverse in the sense that, with the increase in slip parameter, the load carrying capacity and response time decreased. Patel[17] dealt with the effect of velocity slip on the behavior of a squeeze film in a uniform magnetic field between two circular disks. (When the slip parameter increased, the load carrying capacity was found to decrease. The effect of velocity slip on the squeeze film behavior between rotating rough porous circular plates with concentrated circular pockets was investigated Thakkar et al.[28]. It was shown here that the negatively skewed roughness resulted in improved performance at a minimum slip velocity.

Patel and Deheri[19] investigated the effect of slip velocity on the performance of a rough porous slider bearing magnetic fluid-based squeeze film. It was established that load carrying capacity was reduced by the slip velocity but the friction remained unchanged. Analyzed the effect of slip velocity on a short porous bearing based on ferrofluid Patel and Deheri[21]. Here, there was a narrow option for the magnetic strength to reduce the adverse effect of slip velocity. The magnetic force had a narrow option here to reduce the adverse effect of slip velocity. In fact, effects of variation in viscosity and velocity were analyzed in the squeeze film lubrication of two circular plates. The slip velocity resulted in reduced capacity for load carrying while higher viscosity provided increased capacity for load carrying.

The stochastic theory of hydrodynamic lubrication of rough surfaces Prakash and Tiwari[24] was used to study the effect of surface roughness on the response of a squeeze film between two circular plates when one plate had a porous face. It has been established here that the roughness has significantly affected the system. Prajapati[22] analyzed the combined effect of surface roughness and deformation on the film squeeze behavior between rotating circular porous plates with a concentric circular pocket. The pocket introduction reduced the bearing's load carrying capacity. Patel and Deheri[20] modified Prajapati[22] the analysis of ferrofluid-based squeeze film performance between rough porous circular plates with a concentrated circular pocket. Compared to that of Prajapati's configuration, a better performance was recorded here.

Here, the combined effect of surface roughness and velocity slip on the performance of a ferrofluid-based squeeze film in rough porous parallel circular surfaces was analyzed.

**Analysis:**

The configuration of the bearing system is presented in Figure – I.

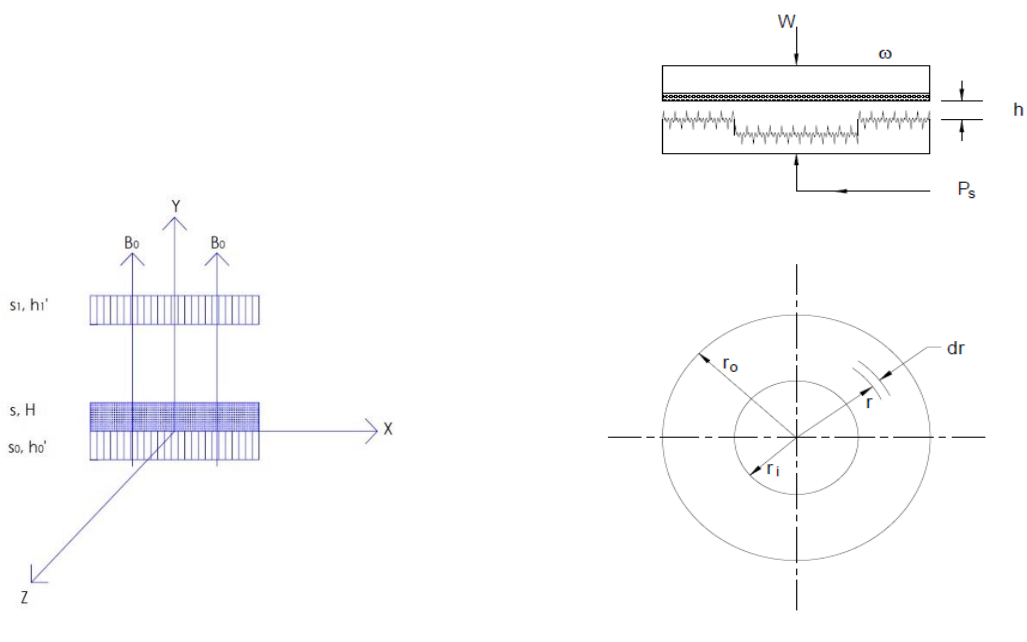


**Figure – I Configuration of bearing system**

Usually the following assumptions are considered for the calculation of different performance characteristics

1. The recess is deep enough for the pressure in it to be uniform
2. The rotational velocity of the bearing is very low and its effect is neglected for the generation of pressure.

Applied a thrust load w as shown in the Figure −I and the bearing supports the metal-free load to metal contact. Within the pocket and land, the load w is supported by the fluid. The fluid escapes by land or sill around the recess in the radial direction through the restrictions. In the light of Christensen and Tonder's discussions [5,6, 7], the bearing surfaces are considered longitudinally rough. The lubricant film's thickness h(x) is determined by

$$h(x) = \bar{h}(x) + h_s \tag{1}$$

Where random roughness h(x) is the mean film thickness and hs is the deviation from the mean film thickness. $h_s$ is considered by nature and governed by the function of probability density $f(h_s)$, $-c \le f(h_s) \le c$ where c is the maximum difference from the mean film thickness. The mean $\alpha$, and standard deviation $\sigma$ and the measure of symmetry $\varepsilon$ of the random variable $h_s$ are defined by the relationships.

$$\alpha = E(h_s)$$

$$\sigma^2 = E\,[(h_s - \alpha)^2]$$

and

$$\varepsilon = E\,[(h_s - \alpha)^3]$$

where E denotes the expected value defined by

$$E(R) = \int_{-c}^{c} R\, f(h_s)\, dh_s \tag{2}$$

The type equation of the Reynolds concerned gives the induced pressure flow for a circular bearing such as ((Majumdar [31], Patel, Deheri, and Vadher [30])

$$Q = -\frac{2\pi r \dfrac{dp}{dr}\left[\dfrac{2}{M^3 m(h)}\left[\dfrac{M}{2} - \tanh\dfrac{M}{2}\right]\right]\left[\dfrac{\phi_0 + \phi_1 + 1}{\phi_0 + \phi_1 + \left(\tanh\dfrac{M}{2}\right)\Big/\left(\dfrac{M}{2}\right)}\right]}{12\mu} \tag{3}$$

where

$$m(h) = h^{-3}\left[1 - 3\alpha h^{-1} + 3h^{-2}(\sigma^2 + \alpha^2) - \frac{3}{40}h^{-3}(\varepsilon + 3\sigma^2\alpha + \alpha^3)\right] (1+4s)/(1+2s)$$

Using Reynolds' boundary conditions

$r = r_o$; $p = 0$;

$r = r_i$; $p = p_s$;

the governing equation for the film pressure p is given by

$$p = p_s \frac{\ln\left(\dfrac{r}{r_o}\right)}{\ln\left(\dfrac{r_i}{r_o}\right)} \tag{4}$$

where in

$$p_s = \frac{6}{\pi\left[\dfrac{2}{M^3 m(h)}\left[\dfrac{M}{2} - \tanh\dfrac{M}{2}\right]\right]\left[\dfrac{\phi_0 + \phi_1 + 1}{\phi_0 + \phi_1 + \left(\tanh\dfrac{M}{2}\right)\Big/\left(\dfrac{M}{2}\right)}\right]}\ln\left(\frac{r_o}{r_i}\right) \tag{5}$$

Introduction of the dimensionless terms

$$P_s^* = \frac{6\ln\left(\frac{1}{k}\right)}{\pi \frac{\left(2/M^3\right)}{M^*(h)}\left[\frac{M}{2} - \tanh\frac{M}{2}\right]\left[\frac{\phi_0+\phi_1+1}{\phi_0+\phi_1+\left(\tanh\frac{M}{2}\right)/\left(\frac{M}{2}\right)}\right]}$$

$$M^*(h) = m\,(h)\ h^3 = \left(1-3\alpha^*+3(\alpha^{*2}+\sigma^{*2}) - \frac{3}{40}(\varepsilon^*+3\sigma^{*2}\,\alpha^*+\alpha^{*3}\right) \bullet (1+4s*)/(1+2s*)$$

$$\alpha^* = \left(\frac{\alpha}{h}\right) \qquad \sigma^* = \left(\frac{\sigma}{h}\right) \qquad \varepsilon^* = \left(\frac{\varepsilon}{h^3}\right) \qquad k = \left(\frac{r_i}{r_o}\right)$$

gaves the way for the expression of pressure distribution in non-dimensional form as

$$P = P_s^* \frac{\ln\left(\frac{r}{r_o}\right)}{\ln\left(\frac{r_i}{r_o}\right)} \tag{6}$$

The load bearing capacity w is calculated by integrating the pressure which takes the dimensionless form

$$W = \frac{P_s^* \ln(1\text{-}k^2)}{\ln\left(\frac{1}{k}\right)} \tag{7}$$

**Results and Discussions:**

The representation of dimensional pressure profile is given in equation (6), while equation (7) governs the non-dimensional load bearing capacity. From these equations, the load carrying capacity is clearly observed

$W \propto P_s^*$

and

$$p_s = \frac{Q}{\frac{\left(2/M^3\right)}{m(h)}\left[\frac{M}{2} - \tanh\frac{M}{2}\right]\left[\frac{\phi_0+\phi_1+1}{\phi_0+\phi_1+\left(\tanh\frac{M}{2}\right)/\left(\frac{M}{2}\right)}\right]}$$

This suggests that the load increases as the average stochastic squeeze film thickness decreases for a constant flow rate. The bearing is therefore self-compensating if the flow rate is considered to be constant. It is shown from equations (6) and (7) that the effect of parameters of conductivity on pressure distribution and load capacity is determined by

$$\frac{\phi_0+\phi_1+\left(\tanh\frac{M}{2}\right)/\left(\frac{M}{2}\right)}{\phi_0+\phi_1+1}$$

which turns to

$$\frac{\phi_0+\phi_1}{\phi_0+\phi_1+1}$$

For large M values because as tanh(M) $\cong$ 1 and (2/M) $\cong$ 0. Furthermore, it is noticed that the capacity of the pressure and load carrying increases with increases in range $\phi_0+\phi_1$ as both functions are increasing functions of $\phi_0+\phi_1$.

Figures (1) to (6) clearly show that the hydromagnetization parameter leads to a sharp increase in the capacity of the load bearing, While Figures (7) to (11) provide the load profile for $\phi_0+\phi_1$ for different standard deviation, variance, skewness, slip parameter and radii ratio values respectively. Here, too, the capacity of load carrying increases as the conductivity parameter increases.

Figures (7) to (11) also indicate that up to some extent the load increases sharply and then this rate of increase becomes slower.

Figures (12) to (15) show that the standard deviation associated with longitudinal roughness causes increased load bearing capacity with different parameters such as variance, skewedness, slip parameter and radius ratio being respected. Figure also describes variation in load carrying capacity for different variance values. (16) to (18). It is noticed from these figures that the load decreases as the positive variance increases while the variance (− ve) increases it. The skewed load capacity trends are similar to the variance observed from Figure (19) to (20). From Figure (21) the load decreases with respect to the aspect ratio while it increases for smaller values of the slip parameter.

This means that this type of bearing system can go a long way to better bearing system performance by combining negative skewed roughness with negative variance.

It is seen that the performance of the bearing is affected by small as well as large values of M when the plates are considered to be conducting electrically, when the plates are taken to be non-conductive, in accordance with the hydromagnetic case. Furthermore, this can be clarified physically by fringing phenomena that occur when the plates are conducting electrically.

**Conclusions:**

The slip parameter deserves to be kept at least for effective bearing system performance. Even in the case of negative skewed roughness, magnetization may not go too far in reducing the adverse effect slip velocity. The roughness aspects must therefore be given priority during the design of the bearing system, even if there is adequate magnetic strength. Moreover, even in the absence of flow, this type of bearing system supports a certain amount of load, which does not occur in conventional lubricant-based bearing systems.

**Fig. 1 Variation of load carrying capacity with respect to M and $\phi_0$ + $\phi_1$**

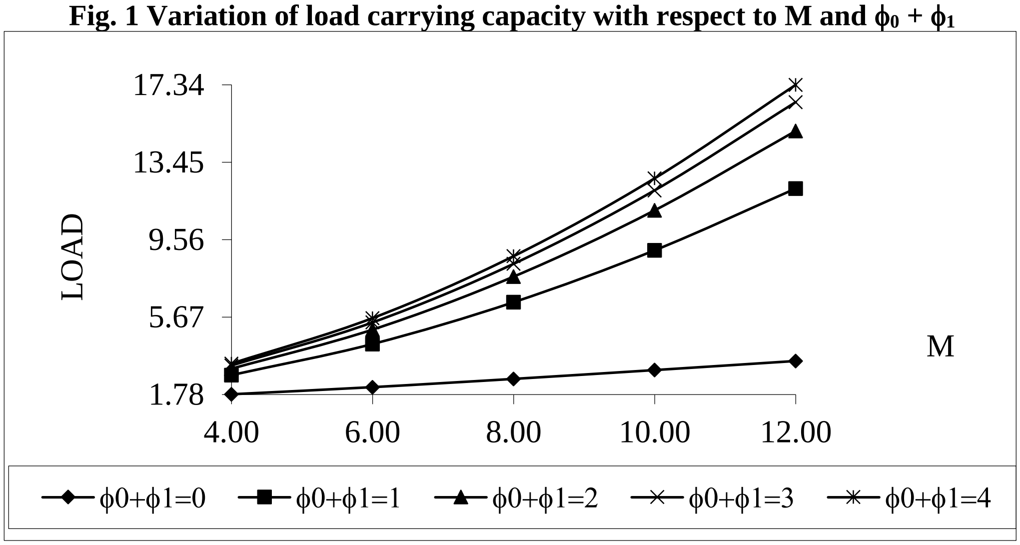

**Fig. 2 Distribution of load bearing capacity with respect to M and σ***

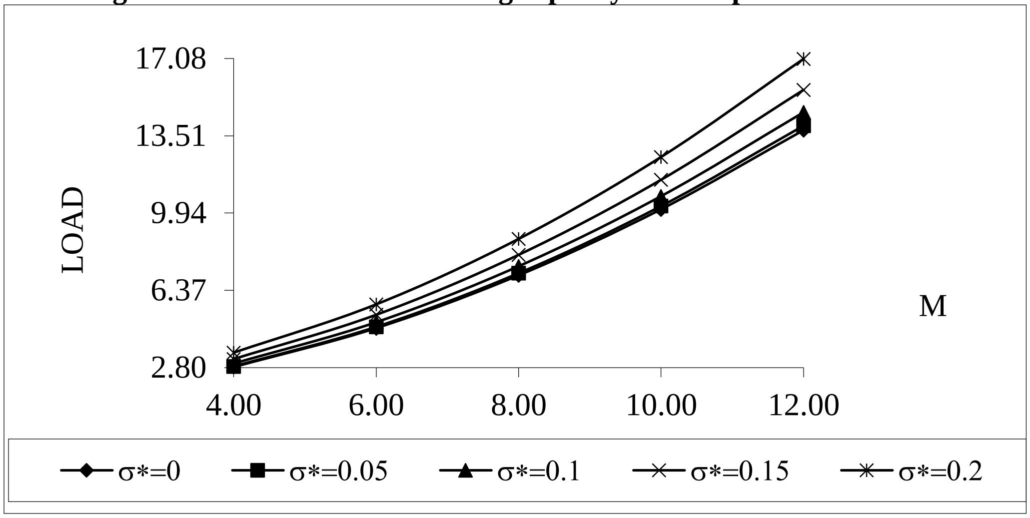


**Fig. 3 Profile of load with respect to M and α***

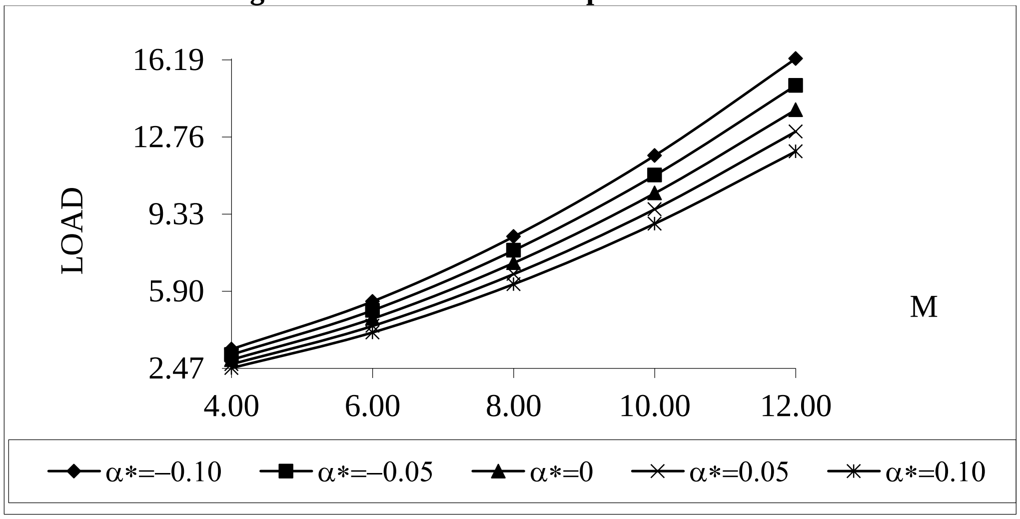


**Fig. 4 Variation of load carrying capacity with respect to M and ε***

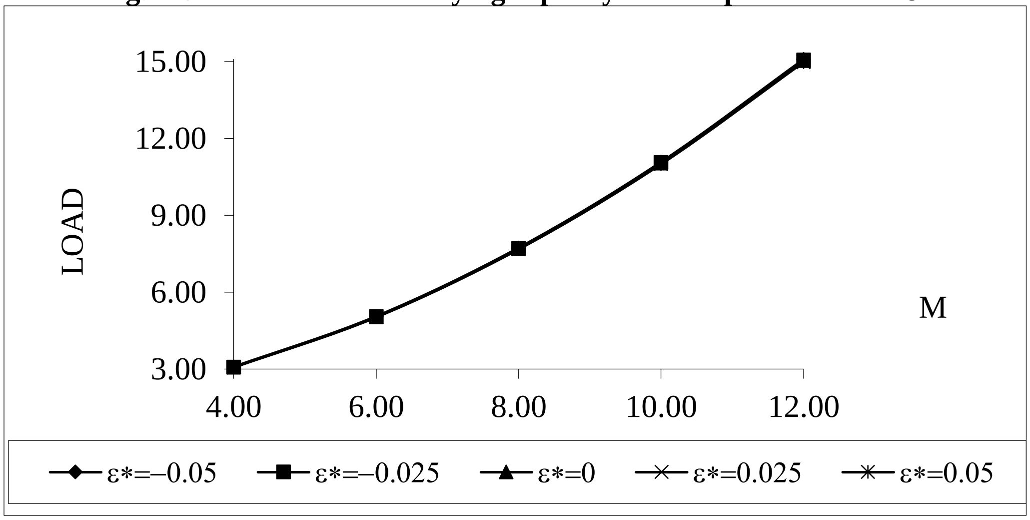

**Fig. 5 Distribution of load bearing capacity with respect to M and k**

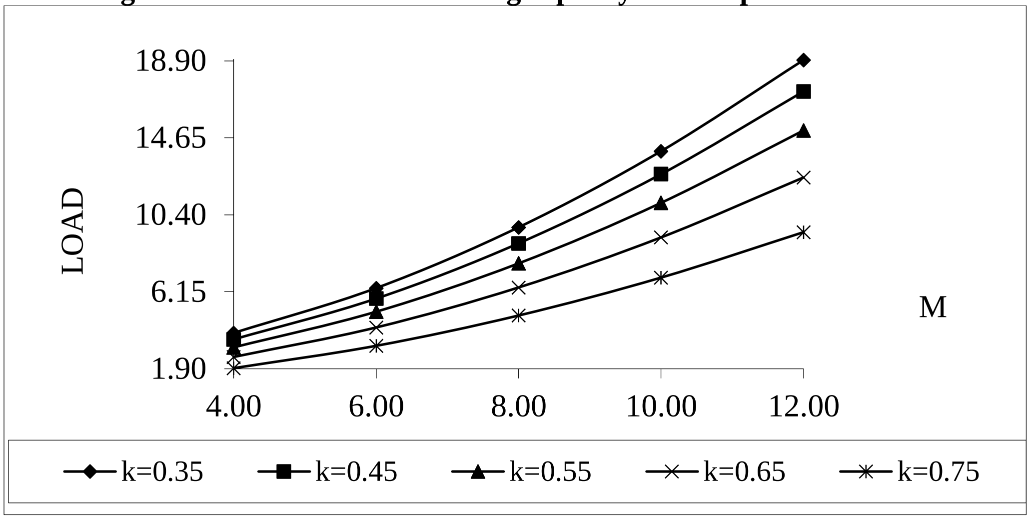


**Fig. 6 Distribution of load bearing capacity with respect to M and s***

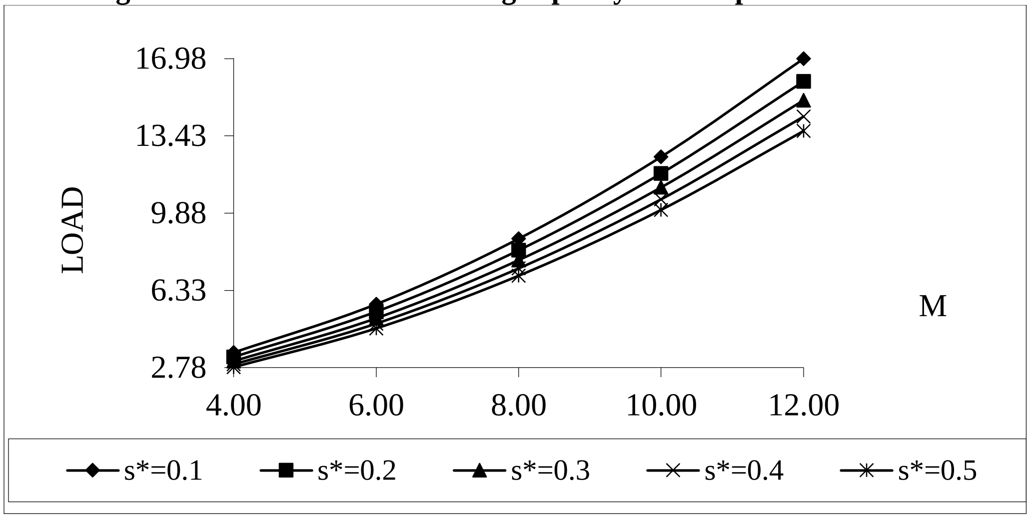


**Fig. 7 Profile of load with respect to $\phi_0 + \phi_1$ and σ***

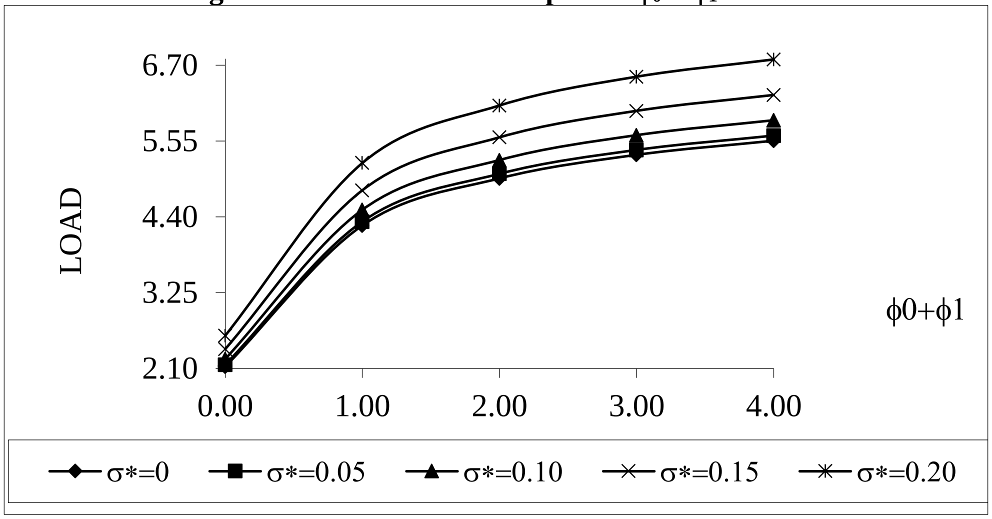

ISSN NO: 0975-6876

**Fig. 8 Variation of load carrying capacity with respect to $\phi_0 + \phi_1$ and $\alpha^*$**

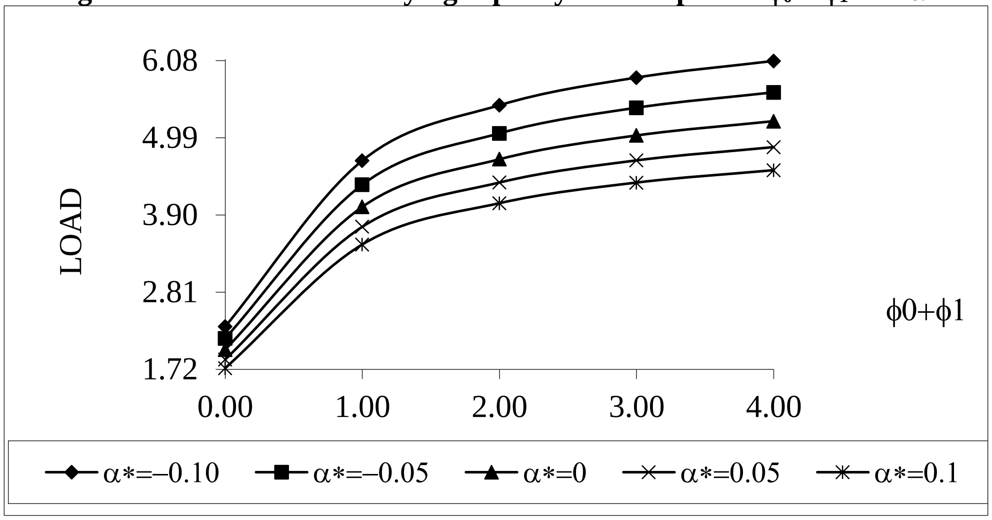


**Fig. 9 Distribution of load bearing capacity with respect to $\phi_0 + \phi_1$ and $\varepsilon^*$**

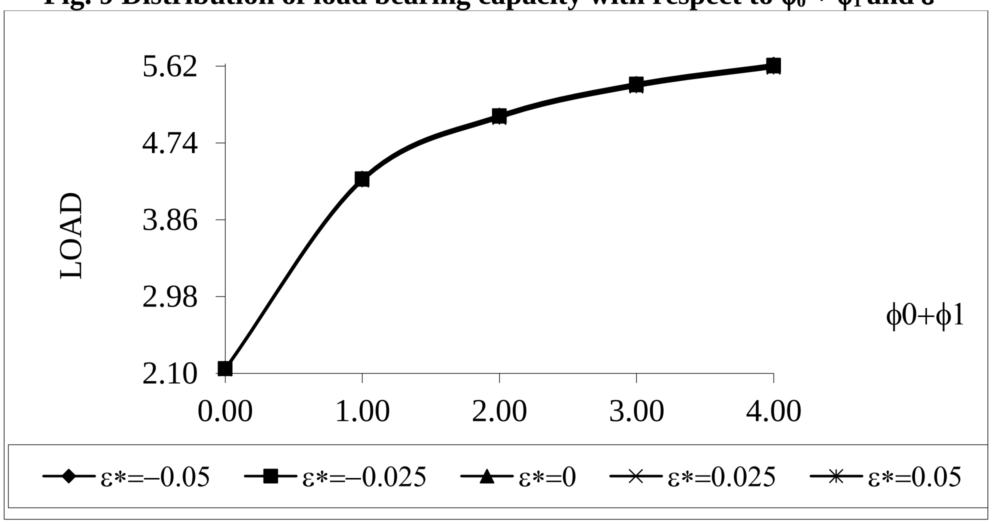


**Fig. 10 Profile of load with respect to $\phi_0 + \phi_1$ and k**

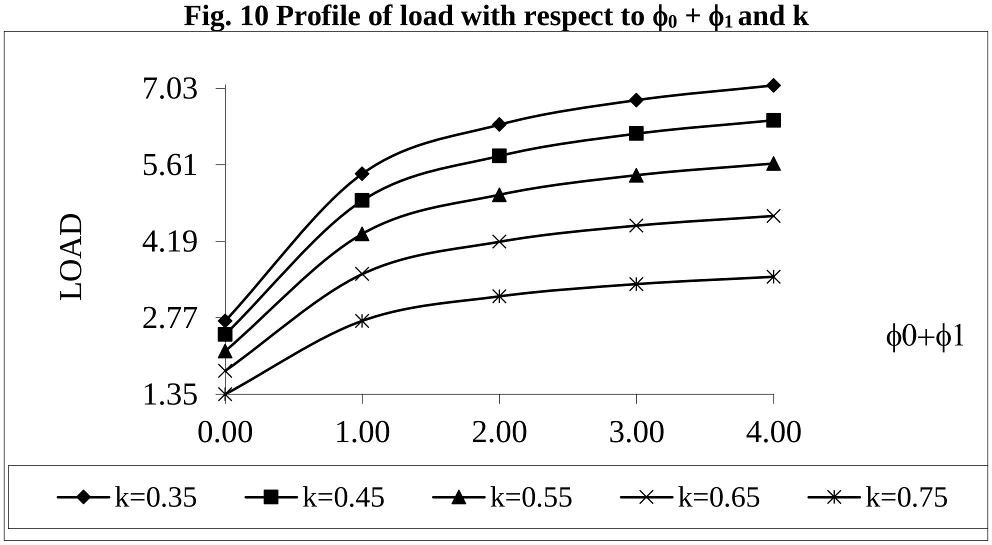

**Fig. 11 Profile of load with respect to $\phi_0 + \phi_1$ and s***

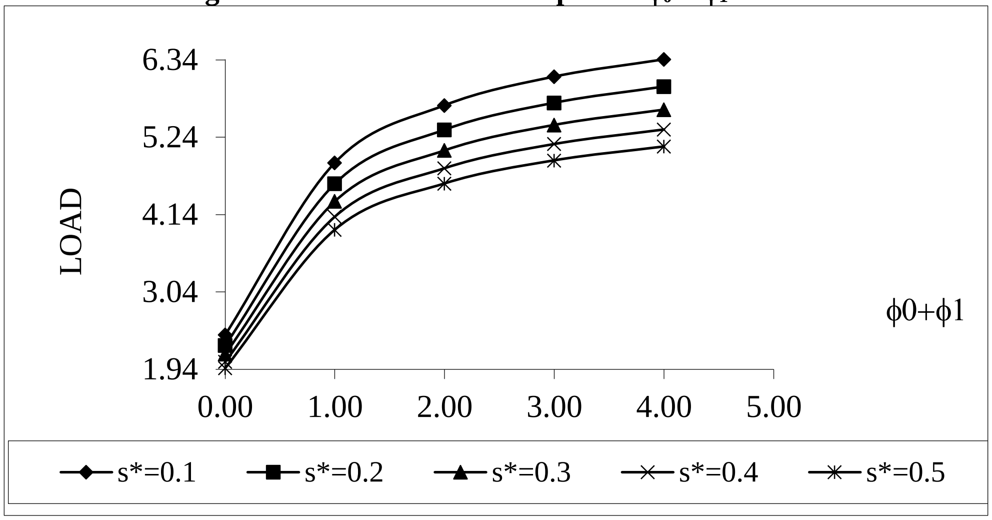


**Figure: 12 Variation of load carrying capacity with respect to σ* and α***

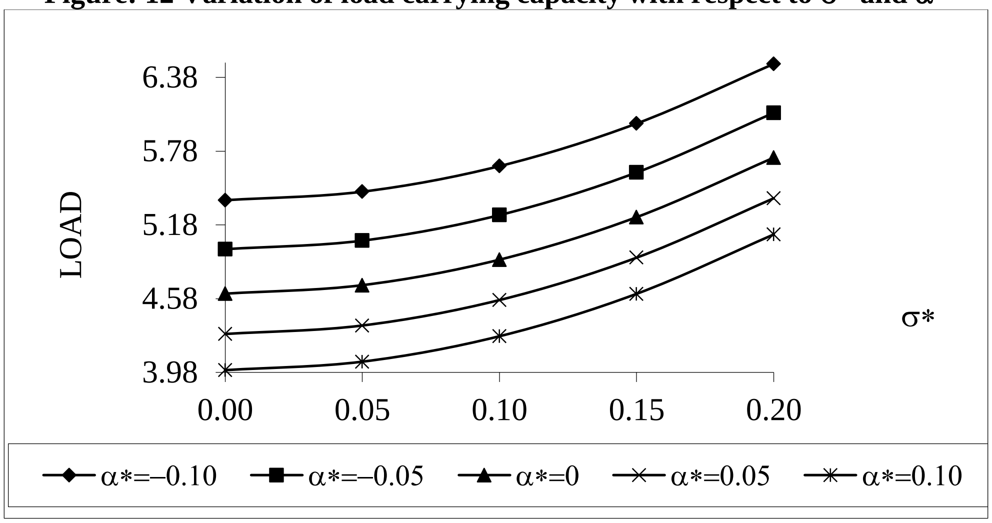


**Fig. 13 Distribution of load bearing capacity with respect to σ* and ε***

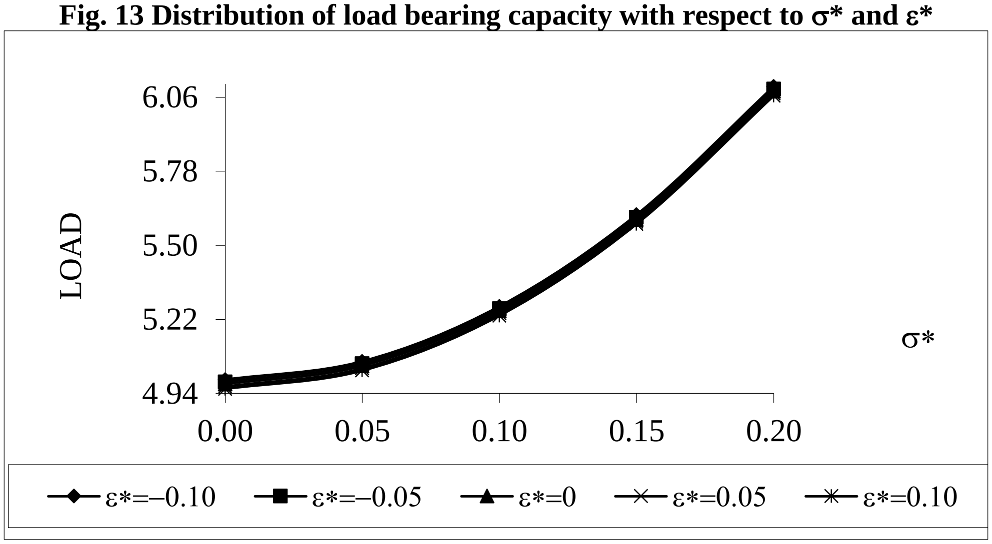

**Fig. 14 Profile of load with respect to σ* and k**

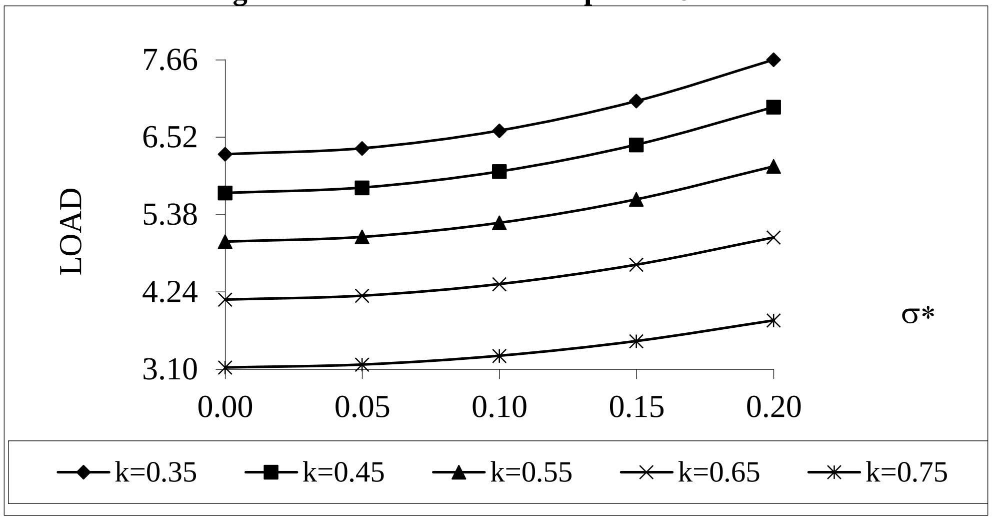


**Fig. 15 Profile of load with respect to σ* and s***

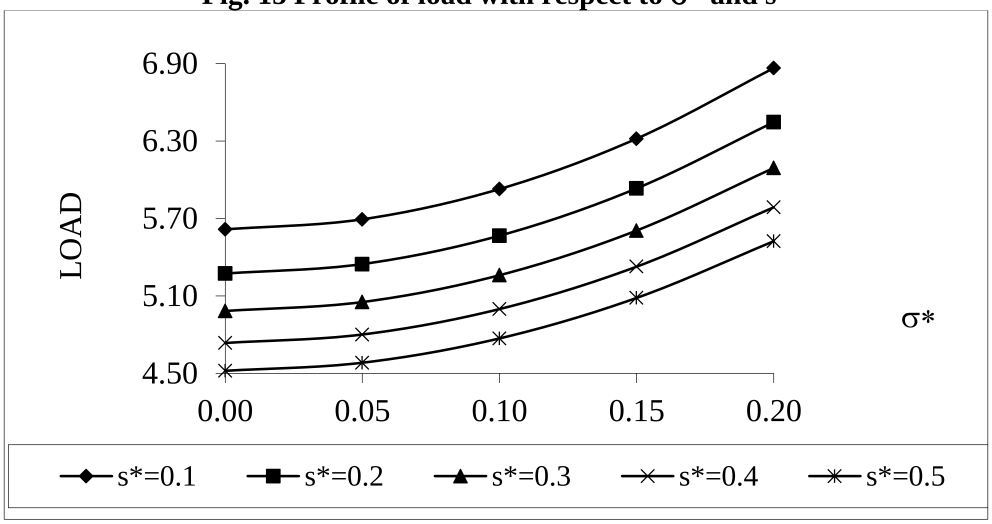


**Fig. 16 Variation of load carrying capacity with respect to α* and ε***

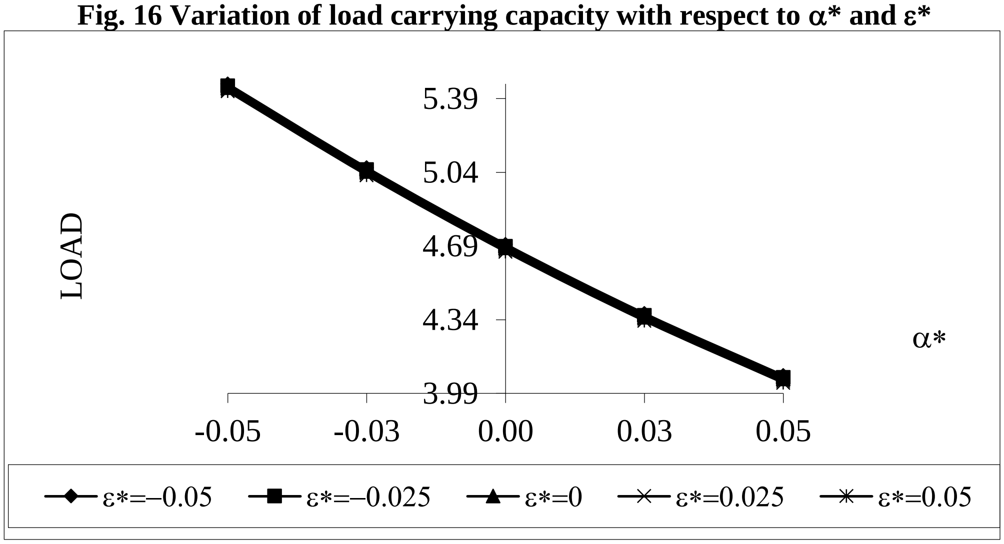

**Fig. 17 Distribution of load bearing capacity with respect to α* and k**

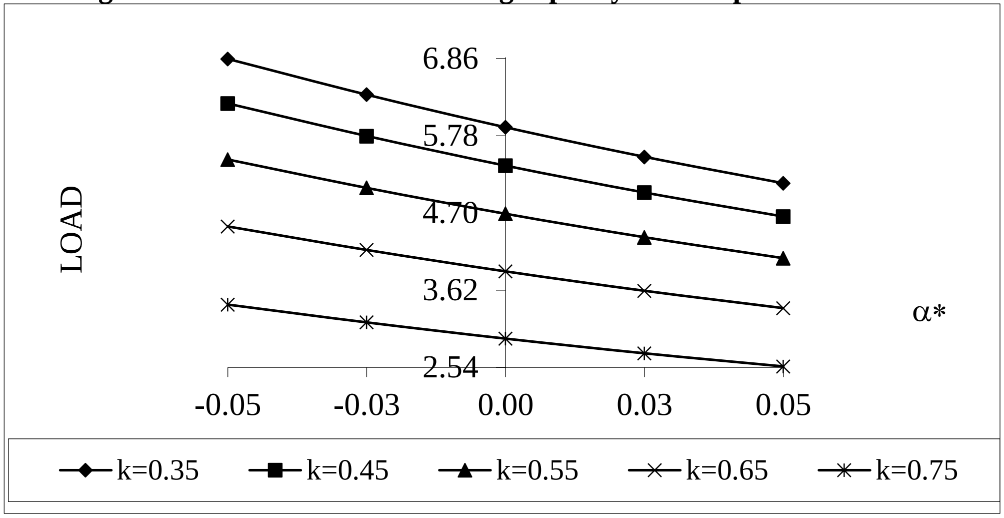


**Fig. 18 Distribution of load bearing capacity with respect to α* and s***

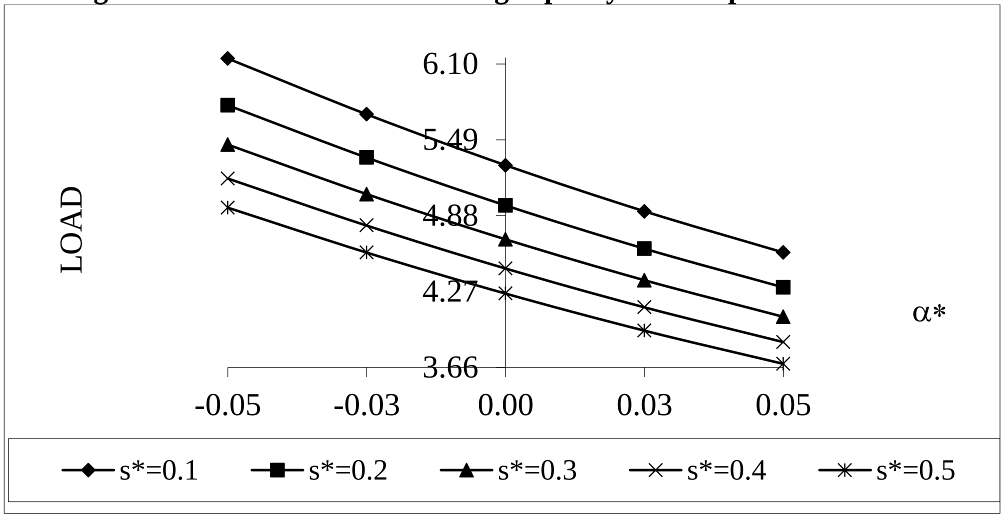


**Fig. 19 Profile of load with respect to ε* and k**

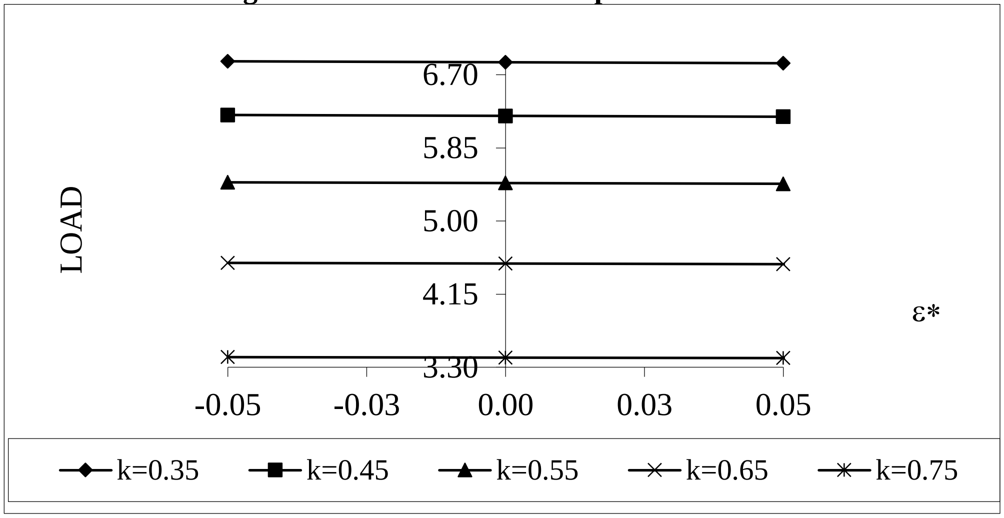

**Fig. 20 Profile of load with respect to ε* and s***

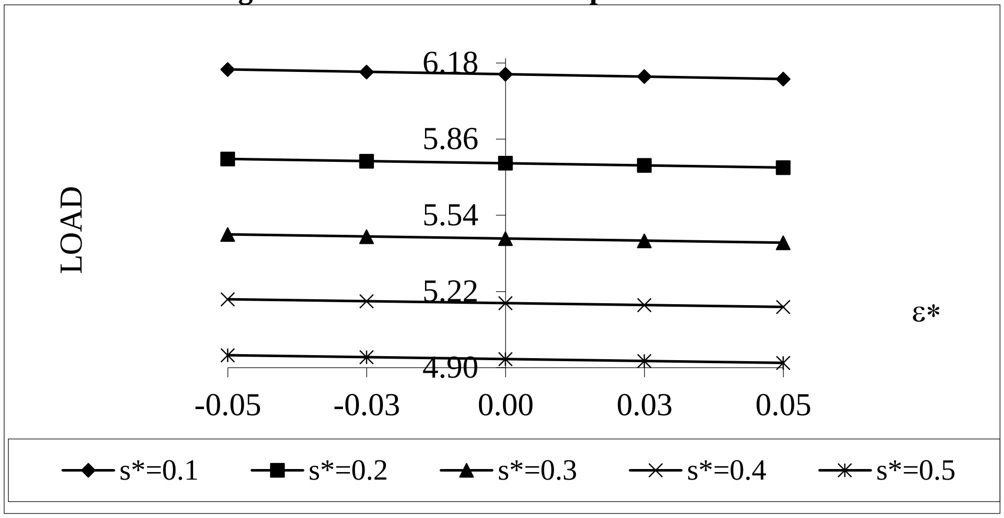


**Fig. 21 Profile of load with respect to k and s***

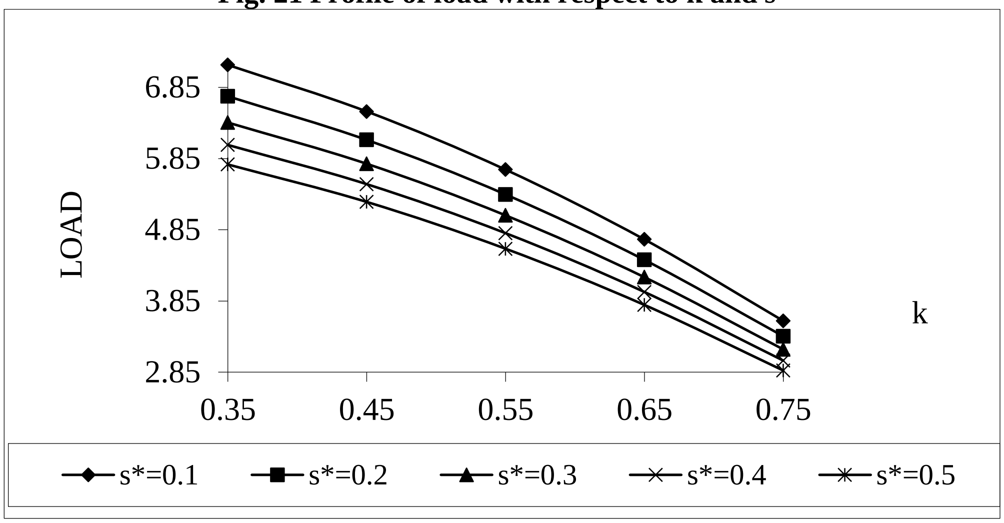


**References:**

1. Beavers, G. S. and Joseph, D. D. “Boundary conditions at a naturally permeable wall”. Journal of Fluid Mechanics, 1967. 30(01): 197.
2. Bhat M.V. “Lubrication with a magnetic fluid”. Team spirit (India) Pvt. Ltd. 2003.
3. Bhat, M. V. and Deheri, G. M. “Porous composite slider bearing lubricated with magnetic fluid”, Japanese Journal of Applied Physics, 1991. 30(1).
4. Bhat, M. V. and Deheri, G. M. “Magnetic-fluid-based squeeze film in curved porous circular discs”. Journal of Magnetism and Magnetic Materials, 1993. 127(1–2): 159-162.
5. Christensen H. and Tonder K. C. “Tribology of rough surfaces: Stochastic models of hydrodynamic lubrication”, SINTEF Report No.10: 1969 a. 69-18.
6. Christensen H. and Tonder K. C. “Tribology of rough surfaces: Parametric study and comparison of lubrication models”, SINTEF Report No.22: 1969 b. 69-18.
7. Christensen H. and Tonder K. C. “The hydrodynamic lubrication of rough bearing surfaces of finite width”. ASME-ASLE lubrication conference, 1970. Paper No.70-Lub-7: October 12-15.
8. Deheri, G. and Abhangi, N. “Magnetic fluid-based squeeze film between curved rough circular plates”. MECHANIKA, 2008. 4(72): 34-39.
9. Deheri, G. and Patel, R. M. “Squeeze Film Based Magnetic Fluid In Between Porous Circular Disks with Sealed Boundary”. Int. J. of Applied Mechanics and Engineering, 2006. 11 (4): 803-812.

10. Deheri, G., Patil, H. and Patel, R. M. “Behavior of Magnetic Fluid Based Squeeze Film between Porous Circular Plates with Porous Matrix of Variable Thickness”. International Journal of Fluid Mechanics Research, 2007. 34 (6): 506-514.
11. Gupta, J. L. and Deheri, G. “Effect of Roughness on the Behavior of Squeeze Film in a Spherical Bearing”. Tribology Transactions, 1996. 39(1): 99-102.
12. Gupta, J. L. and Patel, K. C. “Effect of axial pinch on the porous walled squeeze film with velocity slip”. Wear, 1975. 31(2): 381–389.
13. Hai, W. (1972). Effect of velocity-slip on the squeeze film between porous rectangular Plates. Wear, 20(1): 67–71.
14. Lin, J. R., Lu, R., Lin, M. and Wang, P. “Squeeze film characteristics of parallel circular disks lubricated by ferrofluids with non-Newtonian couple stresses”. Tribology International, 2013. 61: 56–61.
15. Murti, P. R. K. “Squeeze-Film Behavior in Porous Circular Disks”. Journal of Tribology, 1974. 96(2): 206-209.
16. Neuringer, J. L. and Rosensweig, R. E. “Magnetic fluid”. Physics of Fluids, 7(12):19-27.
17. Patel, K. C. (1980). “The hydromagnetic squeeze film between porous circular disks with velocity slip”. Wear, 1964. 58(2): 275–281.
18. Patel, K. C. and Hingu, J. V. “Hydromagnetic squeeze film behavior in porous circular disks”. Wear, 1978. 49(2): 239–246.
19. Patel, N. and Deheri, G. “Effect of Surface Roughness on the Performance of a Magnetic Fluid Based Parallel Plate Porous Slider Bearing with Slip Velocity”. Journal of the Serbian Society for Computational Mechanics, 2011. 5(1): 104-118.
20. Patel, R. M. and Deheri, G. “A study of magnetic fluid-based squeeze film behavior between porous circular plates with a concentric circular pocket and effect of surface roughness”. Industrial Lubrication and Tribology, 2003. 55 (1): 32 – 37.
21. Patel, R. U. and Deheri, G. M. “Effect of Slip Velocity on the Performance of a Short Bearing Lubricated with a Magnetic Fluid”. Acta Polytechnica. Journal of Advanced Engineering, 2013 53(6).
22. Prajapati, B. L. “Squeeze film behavior between rotating porous circular plates with a concentric circular pocket: Surface roughness and elastic deformation effects”. Wear, 1992. 152(2): 301–307.
23. Prajapati, B. L. “On certain Theoretical Studies in Hydrodynamic and Electro-magneto-hydrodynamic Lubrication”. Ph.D. Thesis: Sardar Patel University. Gujarat. 1995.
24. Prakash, J. and Tiwari, K. “Roughness Effects in Porous Circular Squeeze-Plates with Arbitrary Wall Thickness”. Journal of Tribology, 1983. 105(1). 90-95.
25. Prakash, J. and Vij, S.K. “Effect of velocity slip on the squeeze film between rotating porous annular discs”. Wear, 1976. 38(1): 73-85.
26. Rao, R. R., Gouthami, K. and Kumar J. V. “Effects of velocity-slip and viscosity variation in squeeze film lubrication of two circular plates”. Tribology in Industry, 2013. 35(1): 51-60.
27. Sparrow, E. M., Beavers, G. S. and Hwang, I. T. “Effect of Velocity Slip on Porous-Walled Squeeze Films”. Journal of Tribology, 1972. 94(3): 260-264.
28. Thakkar, S., Patil, H., Deheri, G. and Patel, R. M. “Effect of transverse surface roughness on the performance of squeeze film behavior between rotating porous circular plates having concentric circular pocket with velocity slip”. International Colloquiam Tribology, Lubricants, Materials and Lubrication Engineering,: 31 pages. 2008.
29. Tzeng S. T. and Saibel E. “Surface roughness effect on slider bearing lubrication”-Trans ASME, J. Lub. Tech.a, 1967.10: 334-338.
30. Patel, R. M., Deheri, G. M. and Vahdr, P. “Hydromagnetic rough porous circular step bearing”, Eastern Academic Journal, 2015. 3, p.p. 71-87.
31. Majumdar, B. C. “Introduction to tribology of bearing”. Wheeler publishers, Wheeler Co .Ltd. 1985.